A Novel and Efficient Lifting Scheme based Super Resolution Reconstruction for Early Detection of Cancer in Low Resolution Mammogram Images

Liyakathunisa   *liyakath@indiatimes.com*
Ph.D Research Scholar
Dept of Computer Science & Engg
S. J. College of Engineering
Mysore, India.

C.N .Ravi Kumar   *kumarcnr@yahoo.com*
Professor & Head of Department
Dept of Computer Science & Engg
S. J. College of Engineering
Mysore, India.

Abstract

Mammography is the most effective method for early detection of breast diseases. However, the typical diagnostic signs, such as masses and microcalcifications, are difficult to be detected because mammograms are low contrast and noisy images. We concentrate on a special case of super resolution reconstruction for early detection of cancer from low resolution mammogram images. Super resolution reconstruction is the process of combining several low resolution images into a single higher resolution image. This paper describes a novel approach for enhancing the resolution of mammographic images. We are proposing an efficient lifting wavelet based denoising with adaptive interpolation for super resolution reconstruction. Under this frame work, the digitized low resolution mammographic images are decomposed into many levels to obtain different frequency bands. We use Daubechies (D4) lifting schemes to decompose low resolution mammogram images into multilevel scale and wavelet coefficients. Then our proposed novel soft thresholding technique is used to remove the noisy coefficients, by fixing optimum threshold value. In order to obtain an image of higher resolution adaptive interpolation is applied. Our proposed lifting wavelet transform based restoration and adaptive interpolation preserves the edges as well as smoothens the image without introducing artifacts. The proposed algorithm avoids the application of iterative method, reduces the complexity of calculation and applies to large dimension low-resolution images. Experimental results show that the proposed approach has succeeded in obtaining a high-resolution mammogram image with a high PSNR, ISNR ratio and a good visual quality.

Keywords: Adaptive Interpolation, Lifting Wavelet Transform, Mammogram, Super Resolution, Soft Thresholding.

1. INTRODUCTION
Breast cancer is the most common cause of cancer death in women between age of 40 and 45 years. It is one of the leading causes of mortality in women. The World Health Organization's International Agency for Research on Cancer in Lyon, France, estimates that more than 1,50,000 women worldwide die of breast cancer each year [4]. It is expected that 89,000 new cases of breast cancer will be found each year. One out of every 15 newly born girls is expected to develop breast cancer. Mammography, Xeroradiography and Thermography are used for the detection of cancer.

A cancerous tumor in the breast is a mass of breast tissue that is growing in an abnormal, uncontrolled way. The primary signatures of this disease are masses and micro calcifications. Masses are space occupying lesions, described by their shapes, margins and dense properties. Micro calcification is tiny deposits of calcium that appear as small bright spots in the mammogram. Small clusters of micro calcification appearing as collection of white spots on mammograms show an early warning of breast cancer. Primary prevention seems impossible, since the cause of this disease is still remains unknown. An improvement of early diagnostic technique is critical for women's quality of life.

There is a clear evidence which shows that early diagnosis and treatment of breast cancer can significantly increase the chance of survival for patients [5] [6]. The early detection of cancer may lead to proper treatment. Mammography is the main test used for screening and early diagnosis. Mammograms are good at catching infiltrating breast cancer. The current clinical procedure is difficult, time consuming and demands great concentration during reading. Due to large number of normal patients in the screening programs, there is a risk that radiologists may miss some subtle abnormalities.

When a cancer is non-invasive, it is harder to catch with a mammography in women under 50 because of their breast density. Some of the drawbacks of film mammography are, it gives a lot of false negatives. Lumps have an easier time hiding from mammograms in dense breast tissues. The quality of diagnoses depends on the resolution of the mammograms, higher resolutions provides a higher level of detail that normally leads to improved accuracy.

However, to obtain higher resolutions, larger doses of radiation are necessary, which may have harmful effects for patients. Another draw back is that mammograms can be painful and uncomfortable. In order to get a good picture, the technician must apply moderate pressure to the breast. The patient may feel uncomfortable while her breast is being flattened (compressed). To alleviate the above problems we have proposed Super Resolution reconstruction of low resolution mammogram images, in our proposed approach a set of low resolution inputs are used to detect the cancerous tissues, from which a high resolution image is obtained. High Resolution (HR) images give better and accurate results for early detection of cancer in most of the cases. Our proposed approach also lessen the pain and the humiliation that most of the women's faces during mammography. Digital mammography provides the opportunity to apply sophisticated digital processing techniques to aid in screening.

Digital mammography systems have the ability to reprocess the images with mathematical settings that enhance the images. Dense tissues can be seen more clearly through digital enhancements. In recent years several research groups have started to address the goal of resolution augmentation in medical imaging as software post processing challenge. The motivation for this initiative emerged following major advances in the domains of image and video processing that indicated the possibility of enhancing the resolution using Super Resolution algorithms. Super Resolution deals with the task of using several low resolution images from a particular imaging system to estimate, or reconstruct, the high resolution image.

The flow of the topics is as follows; in section II we provide a brief review of the SR algorithm for medical imaging. In section III Mathematical Formulation for Super Resolution Model is created and described in the context of mammographic images, section IV presents the Lifting schemes, in section V the Proposed method for super resolution reconstruction of LR mammogram images is discussed, section VI provide the proposed Super Resolution Reconstruction algorithm, Experimental results are presented and discussed in section VII and finally section VIII consists of conclusion.

2. RELATED WORK

Super Resolution problem was extensively addresses in the literature during the last two decades. A variety of reconstruction algorithm have been proposed in literature, where the common goal is to estimate the HR image as accurately as possible, while minimizing the noise, and preserving the image smoothness. In 2001 and 2003 initial attempts were made to adapt super resolution algorithms from the computer vision community to medical imaging applications, initial research dealt with Magnetic Resonance Imaging (MRI) and Position Emission Tomography (PET) modality. Results were encouraged and were reproduced around the world. In this paper we will discuss the main reconstruction algorithms that are in use, such as Iterative Back Projection (IBP)[7] , Projection on to Convex Sets(POCS)[10], Frequency Domain Techniques[8][9] . Green Span and Peled [11] and Kennedy et. al [12] suggested Super Resolution Reconstruction for MRI images where they used IBP. In the IBP approach, an estimate of the high resolution image is compared with low resolution image estimates. The differences between the estimated low resolution images and the actual low resolution images are then used to refine the high resolution image in an iterative manner. Hsu et al. [13] proposed to create high resolution cardiovascular images using a super resolution method based on Projection on Convex Sets (POCS). In the POCS approach, a convex constraint set is set up to maintain consistency with the low resolution images. The estimated high resolution image is projected onto each constraint within the convex constraint set until the desired condition is satisfied. Frequency domain technique was suggested by Tsai and Huang [8] and Kim et al [9]; most frequency domain methods are based on transforming the input images to the frequency domain (using 2-D discrete Fourier transform (DFT)), combining the spectral data and returning the output image. (After applying 2-D IDFT) Phase adaptive Super resolution was proposed by Alexander et al [14] in 2009. In this approach the SR problem is formulated as a constrained optimization problem using a third order Markov prior model, and adapts the priors based on the phase variations of the LR mammographic images. In 2010 super resolution for mammograms was proposed by Jun et al. [15]. In their approach, the algorithm combines machine learning methods and stochastic search to learn the mapping from LR to HR mapping using a data set of training images. In this paper we have proposed a novel and efficient wavelet based super resolution reconstruction of low resolution mammogram images.

3. MATHEMATICAL FORMULATION FOR THE SUPER RESOLUTION MODEL

In this section we give the mathematical model for super resolution image reconstruction from a set of Low Resolution (LR) mammographic images. During acquisition image is often corrupted by noise and because of the slight difference in X-ray attenuation between masses, the images may appear with low contrast and often very blurred. They are also down sampled and wrapped, resulting in a set of aliased, blurred, noisy and shifted (mis -registered) images. In practice the image shifts can be obtained by the x-ray tube rotations or by moving the imaged object with respect to the x-ray source.

Let us consider the low resolution sensor plane by $M_1 \, by \, M_2$. The low resolution intensity values are denoted as $\{y(i,j)\} \, where \, i = 0 \ldots M_1 -1 \, and \, j = 0 \ldots M_2 -1$; if the down sampling parameters are $q_1 \, and \, q_2$ in horizontal and vertical directions, then the high resolution image will be of size $q_1 M_1 \times q_2 M_2$. We assume that $q_1 = q_2 = q$ and therefore the desired high resolution image Z will have intensity values $\{z(k,l)\}$ where $k = 0 \ldots qM_1 -1 \, and \, l = 0 \ldots qM_2 -1$.

Given $\{z(k,l)\}$ the process of obtaining down sampled LR aliased image $\{y(i,j)\}$ is

$$y(i,j) = \frac{1}{q^2} \sum_{k=qi}^{(q+1)i-1} \sum_{l=qj}^{(q+1)j-1} z(k,l) \qquad (1)$$

i.e. the low resolution intensity is the average of high resolution intensities over a neighborhood of q^2 pixels. We formally state the problem by casting it in a Low Resolution restoration frame work.

There are P observed images $\{Y_m\}_{m=1}^{p}$ each of size $M_1 \times M_2$ which are decimated, blurred and noisy versions of a single high resolution image Z of size $N_1 \times N_2$ where $N_1 = qM_1$ and $N_2 = qM_2$.

After incorporating the blur matrix, and noise vector, the image formation model is written as

$$Y_m = H_m DZ + \eta_m \qquad \text{Where m=1...P} \qquad (2)$$

here D is the decimation matrix of size $M_1 M_2 \times q^2 M_1 M_2$, H is PSF of size $M_1 M_2 \times M_1 M_2$, η_m is $M_1 M_2 \times 1$ noise vector and P is the number of low resolution observations Stacking P vector equations from different low resolution images into a single matrix vector

$$
\begin{bmatrix} y_1 \\ . \\ . \\ . \\ y_p \end{bmatrix} = \begin{bmatrix} DH_1 \\ . \\ . \\ DH_p \end{bmatrix} Z + \begin{bmatrix} \eta_1 \\ . \\ . \\ . \\ \eta_p \end{bmatrix} \qquad (3)
$$

the matrix D represents filtering and down sampling process of dimensions $q^2 M_1 M_2 \times 1$ where q is the resolution enhancement factor in both directions. Under separability assumptions, the matrix D which transforms the $qM_1 \times qM_2$ high resolution image to $N_1 \times N_2$ low resolution images where $N_1 = qM_1$, $N_2 = qM_2$ is given by

$$D = D_1 \otimes D_1 \qquad (4)$$

where $\otimes$ represents the kronecker product, and the matrix D_1 represents the one dimensional low pass filtering and down sampling. When q=2 the matrix D_1 will be given by

$$
D_1 = \frac{1}{2} \begin{bmatrix} 11\ 00\ 00\ .....00 \\ 00\ 11\ 00......00 \\ :\ \ :\ \ :\ \ \ \ \ \ : \\ :\ \ :\ \ :\ \ \ \ \ \ : \\ 00\ \ 00\ \ \ \ \ \ \ 11 \end{bmatrix} \qquad (5)
$$

and

$$
D = \frac{1}{2^2} \begin{bmatrix} 11\ 00\ 00\ .....00 \\ 00\ 11\ 00......00 \\ :\ \ :\ \ :\ \ \ \ \ : \\ :\ \ :\ \ :\ \ \ \ \ : \\ 00\ \ 00\ \ \ \ \ \ 11 \end{bmatrix} \qquad (6)
$$

the square matrix H of dimensions $PN_1 \times PN_2$ represents intra channel and inter channel blur operators. i.e. 2D convolution of channel with shift-invariant blurs. The blur matrix is of the from

$$H_I = \begin{bmatrix} H_{(0)} & H_{(1)} & .... & H_{(M-1)} \\ H_{(M-1)} & H_{(0)} & .... & H_{(M-2)} \\ : & : & .... & : \\ : & : & .... & : \\ H_{(1)} & H_{(2)} & .... & H_{(0)} \end{bmatrix}$$

(7)

and it is circulant at the block level. In general each $H_{(i)}$ is an arbitrary $PM_1 \times PM_2$, but if shift invariant circular convolution is assumed $H_{(i)}$ becomes

$$H_{(i)} = \begin{bmatrix} H_{(i,0)} & H_{(i,1)} & .... & H_{(i,M-1)} \\ H_{(i,M-1)} & H_{(i,0)} & .... & H_{(i,M-2)} \\ : & : & .... & : \\ : & : & .... & : \\ H_{(i,1)} & H_{(i,2)} & .... & H_{(i,0)} \end{bmatrix}$$

(8)

which is also circulant at the block level $H_{(i,j)}$. Each $P \times P$ sub matrix (sub blocks) has the form

$$H_{(i,j)} = \begin{bmatrix} H_{11(i,j)} & H_{12(i,j)} & .... & H_{ip(i,j)} \\ H_{21(i,j)} & H_{22(i,j)} & .... & H_{2p(i,j)} \\ : & : & .... & : \\ : & : & .... & : \\ H_{p1(i,j)} & H_{p2(i,j)} & .... & H_{pp(i,j)} \end{bmatrix}$$

(9)

where $H_{ii(m)}$ is intra channel blurring operator, $H_{ij(m)} i \neq j$ is an inter channel blur i.e. P x P non circulant blocks are arranged in a circulant fashion, it's called Block Semi-Block Circulant (BSBC); which can be easily solved using blind deconvolution or regularization.
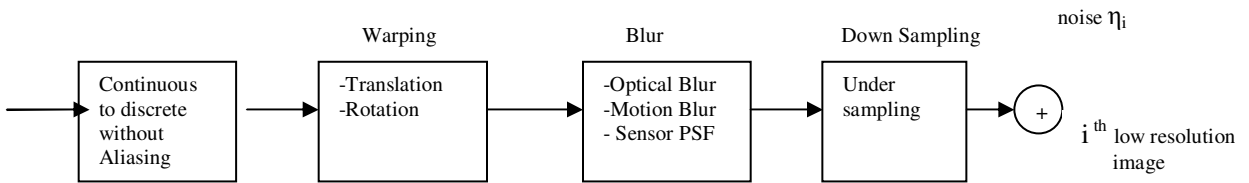

**FIGURE 1:** Low Resolution Observation Model
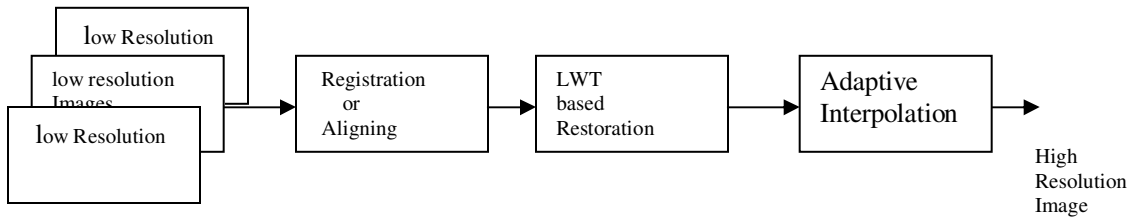
FIGURE 2: Super Resolution Reconstruction Model

4. LIFTING SCHEMES

Wavelet algorithms are recursive. The output of one step of the algorithm becomes the input for the next step. The initial input data set consists of 2n elements. Each successive step operates on 2n-i elements, where i = 1 ... n-1. For example, if the initial data set contains 128 elements, the wavelet transform will consist of seven steps on 128, 64, 32, 16, 8, 4, and 2 elements. In this case $step_{j+1}$ follow $step_j$. If element i in step j is being updated, the notation is $step_{j,i}$. The forward lifting scheme wavelet transform divides the data set being processed into an even half and an odd half. In the notation below $even_i$ is the index of the ith element in the even half and odd_i is the ith element in the odd half (even and odd halves are both indexed from 0). Viewed as a continuous array (which is what is done in the software) the even element would be a[i] and the odd element would be a [i+ (n/2)]. The wavelet Lifting Scheme is a method for decomposing wavelet transforms into a set of stages. Lifting scheme algorithms have the advantage that they do not require temporary arrays in the calculation steps, as is necessary for some versions of the Daubechies D4 wavelet algorithm[16]. The simplest version of a forward wavelet transform expressed in the Lifting Scheme is shown in Figure 3. The predict step calculates the wavelet function in the wavelet transform. This is a high pass filter. The update step calculates the scaling function, which results in a smoother version of the data (low pass filter) [16].
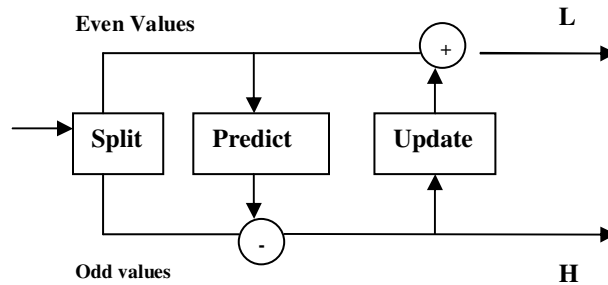

FIGURE 3: Lifting Scheme Forward Wavelet Transform

Predict The predict step uses a function that approximates the data set. The difference between the approximation and the actual data replaces the odd elements of the data set. The even elements are left unchanged and become the input for the next step in the transform. The predict step, where the odd value is "predicted" from the even value is described by the equation.

$$odd_{j+1,i} = odd_{j,1} - P(even_{j,i}) \tag{10}$$

The inverse predicts transform adds the prediction value to the odd element (reversing the prediction step of the forward transform). In the inverse transform the predict step is followed by a merge step which interleaves the odd and even elements back into a single data stream.

Update: The update phase follows the predict phase. The original value of the odd elements has been overwritten by the difference between the odd element and its even "predictor". So in calculating an average the update phase must operate on the differences that are stored in the odd elements. The update step replaces the even elements with an average. These results in a smoother input for the next step of the next step of the wavelet transform. The odd elements also represent an approximation of the original data set, which allows filters to be constructed.

$$even_{j+1,i} = even_{j,i} + U(odd_{j+1,i}) \tag{11}$$

4.1 A Lifting Scheme Version of the Daubechies (D4) Transform

Lifting scheme wavelet transforms are composed of update and predict steps. In this case a normalization step has been added as well.
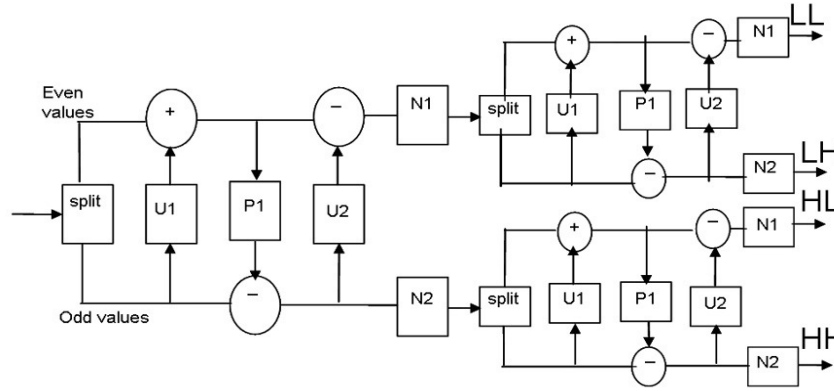
FIGURE 4: Two stage Daubechies D4 Forward lifting Wavelet Transform

The split step divides the input data into even elements which are stored in the first half of an N element array section (S_0 to S_{half-1}) and odd elements which are stored in the second half of an N element array section   (S_{half} to $S_{N\,-1}$). In the forward transform equations below the expression S [half+n] references an odd element and S[n] references an even element. The LL represents the low frequency components and LH, HL, HH are the high frequency components in the horizontal, vertical and diagonal directions.

The forward step equations are

Update1 (U1):
 For n= 0 to half -1

$$S[n] = S[n] + \sqrt{3}S[half + n] \tag{12}$$

Predict (P1):

$$S[half] = S[half] - \frac{\sqrt{3}}{4}S[0] - \frac{\sqrt{3}-2}{4}S[half - 1]$$

$$\tag{13}$$

for n=1 to half -1

$$S[half + n] = S[half + n] - \frac{\sqrt{3}}{4}S[n] - \frac{\sqrt{3}-2}{4}S[n - 1] \tag{14}$$

Update2 (U2):

for n=0 to half -2

$$S[n] = S[n] - S[half + n + 1]$$
$$S[half - 1] = S[half - 1] - S[half] \tag{15}$$

Normalize (N):
for n=0 to half-1

$$S[n] = \frac{\sqrt{3}-1}{\sqrt{2}} S[n]$$

$$S[n+half] = \frac{\sqrt{3}+1}{\sqrt{2}} S[n+half]$$

(16)

the inverse transform is a mirror of the forward transform, in which addition and subtraction operations interchanged.
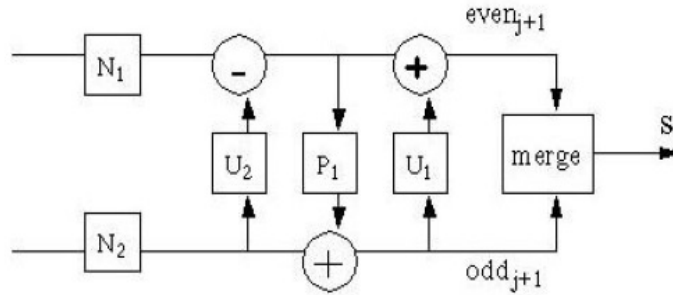
FIGURE 5: Daubechies D4 Inverse Lifting Wavelet Transform

5. PROPOSED SUPER RESOLUTION RECONSTRUCTION OF LOW RESOLUTION MAMMOGRAM IMAGES

Our Low Resolution mammogram images consist of the degradations such as geometric registration wrap, sub sampling, blurring and additive noise. Based on these phenomena our implementation consists of the following consecutive steps.

Step 1: Image registration, which means estimating the geometrical registration wrap between different images.
Step 2: Fusion and Restoration of the registered low resolution images using our proposed efficient Lifting scheme based denoising.
Step 3: Adaptive interpolation of the resulting image from step 2 to obtain a super resolution Mammogram image.

5.1 Image Registration
For super resolution reconstruction, image registration is performed first in order to align the LR images as accurately as possible. It is a process of overlaying two or more images of the same scene taken at different times, from different view points and or by different sensors. Typically one image called the base image is considered the reference to which the other images called input images are compared. The objective is to bring the input image into alignment with the base image by applying a spatial transformation to the input image. Spatial transformation maps locations in one image into a new location in another image. Image registration is an inverse problem as it tries to estimate from sampled images Y_m, the transformation that occurred between the views Z_m considering the observation model of Eq(2). It is also dependent on the properties of the camera used for image acquisition like sampling rate (or resolution) of sensor, the imperfection of the lens that adds blur, and the noise of the device. As the resolution decreases, the local two dimensional structure of an image degrades and an exact registration of two low resolution images becomes increasingly difficult. Super resolution reconstruction requires a registration of high quality. Different methods exists for estimating the motion or sub pixel shift between the two images[17].The registration technique considered in our research is a modified

phase correlation based on Fast Fourier Transform proposed by Fourier Mellin and DeCastro [18].

The transformation considered in our research is rotation, translation and shift estimation. Let's consider the translation estimation, the Fourier transform of the function is denoted by $F\{f(x,y)\}$ or $\hat{f}(w_x, w_y)$. The shift property of the Fourier transform is given by

$$F\{f(x+\Delta x, y+\Delta y)\} = \hat{f}(w_x, w_y)e^{i(w_x \Delta x + w_y \Delta y)}$$

(17)

Eq (17) is the basis of the Fourier based translation estimation algorithms. Let $I_1(x, y)$ be the reference image and $I_2(x, y)$ is the translated version of the base image, i.e

$$I_1(x, y) = I_2(x + \Delta x, y + \Delta y)$$

(18)

by applying the Fourier transform on both the sides of Eq (18). We get

$$\hat{I}_1(w_x, w_y) = \hat{I}_2(w_x, w_y)e^{i(w_x \Delta x + w_y \Delta y)}$$

(19)

or equivalently,

$$\frac{\hat{I}_1(w_x, w_y)}{\hat{I}_2(w_x, w_y)} = e^{i(w_x \Delta x + w_y \Delta y)}$$

(20)

$$corr(x, y) \cong F^{-1}\left(\frac{\hat{I}_1(w_x, w_y)}{\hat{I}_2(w_x, w_y)}\right) = \delta(x + \Delta x, y + \Delta y)$$

(21)

for discrete images we replace the FT in the computation above with FFT, and $\delta(x + \Delta x, y + \Delta y)$ is replaced by a function that has dominant maximum at $(\Delta x, \Delta y)$ as

$$(\Delta x, \Delta y) = \arg\max\{corr(x, y)\}$$

(22)

calculate the cross power spectrum by taking the complex conjugate of the second result. Multiplying the FT together element wise, and normalizing this product element wise.

$$corr(w_x, w_y) \cong \frac{\hat{I}_1(w_x, w_y)}{\hat{I}_2(w_x, w_y)} \bullet \left|\frac{\hat{I}_1(w_x, w_y)}{\hat{I}_2(w_x, w_y)}\right|$$

(23)

$$corr(w_x, w_y) = R \cong \frac{\hat{I}_1(w_x, w_y)\hat{I}_2^*(w_x, w_y)}{\left|\hat{I}_2(w_x, w_y)\right|\left|\hat{I}_1^*(w_x, w_y)\right|} = e^{i(w_x \Delta x + w_y \Delta y)}$$

(24)

where * denotes the complex conjugate. Obtain the normalized cross correlation by applying the inverse FT. i.e. $r = F^{-1}\{R\}$, determine the location of the peak in r. This location of the peak is exactly the displacement needed to register the images

$$(\Delta x, \Delta y) = \arg\max\{r\} \tag{25}$$

The angle of rotation is estimated by converting the Cartesian coordinates to log polar form. We observe that the sum of a cosine wave and a sine wave of the same frequency is equal to phase shifted cosine wave of the same frequency. That is if a function is written in Cartesian form as

$$v(t) = A\cos(t) + B\sin(t) \tag{26}$$

then it may also be written in polar form as

$$v(t) = c\cos(t - \varphi) \tag{27}$$

we may write the Eq (27) in polar form as

$$Y = y(x) = \frac{a_0}{2} + \sum_{k=1}^{N} m_k \cos(2\pi f_k x - \varphi_k) \tag{28}$$

where

$$m_k = \sqrt{a_k^2 + b_k^2} ....(magnitude)$$

$$\varphi_k = \tan^{-1}\left(\frac{b_k}{a_k}\right) ....(Phase)$$

(29)

The Shift is estimated by finding cross power spectrum and computing Eq.(20). We obtain the normalized cross correlation by applying the inverse FT. i.e. $r = F^{-1}\{R_2\}$, determines the location of the peak in r. This location of the peak is exactly the shift $I(x_0, y_0)$ needed to register the images. Once we estimated the angle of rotation, translation and shift, a new image is constructed by reversing the angle of rotation translation and shift.

(a)   (b)
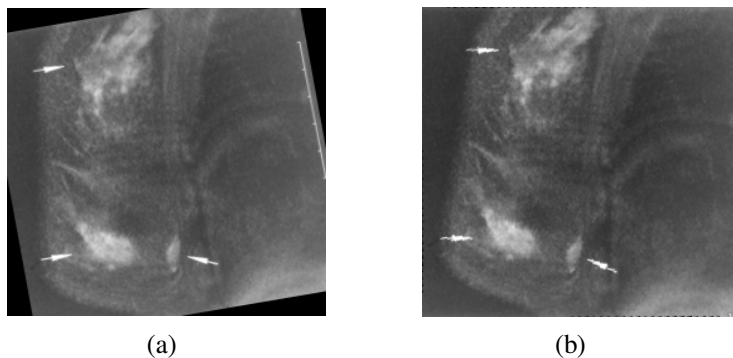
FIGURE 6: (a) Rotated, shifted Mammogram Image (b) Registered Mammogram Image

In the second phase the low resolution registered images are fused using fusion rule, then restoration is performed using our proposed novel denoising technique. In the final phase proposed adaptive interpolation is performed to obtain an image with double, quadrupled the resolution of the original.

5.2 Lifting Wavelet based Restoration

Images are obtained in areas ranging from everyday photography to astronomy, remote sensing, medical imaging and microscopy. In each case there is an underlying object or scene we wish to observe, the original or the true image is the ideal representation of the observed scene. Yet the observation process is never perfect, there is uncertainty in the measurement occurring as blur, noise and other degradations in the recorded images. Image restoration aims to recover an estimate of the original image from the degraded observations. Classical image restoration seeks an estimate of the true image assuming the blur is known, whereas blind image restoration tackles the much more difficult but realistic problem where the degradations are unknown.

The low resolution observation model of Eq.(2) is considered. We formally state by casting the problem in multi channel restoration format, the blur is considered as between channels and within channel of the low resolution images. In order to remove the blur and noise from the LR images we have proposed an efficient wavelet based denoising using thresholding, our proposed approach performs much better when compared to other approaches.

5.2.1. Proposed Efficient lifting Wavelet Transform Based Denoising for SRR Using Thresholding

Image denoising techniques are necessary to remove random additive noises while retaining as much as possible the important image features. The main objective of these types of random noise removal is to suppress the noise while preserving the original image details [19]. Statistical filter like average filter, wiener filter can be used for removing such noises but wavelet based denoising techniques proved better results than these filters. The wavelet transforms compresses the essential information in an image into a relatively few, large coefficients which represents image details at different resolution scales. In recent years there has been a fair amount of research on wavelet thresholding and threshold selection for image denoising [20][21][22] .

Let Z be an M x M image from Eq. (2), during transmission the image Z is corrupted by zero mean White Gaussian noise η with standard deviation σ . At the receiver end the noisy observation Y of Eq. (2) is obtained. The goal is to obtain the image Z from noisy observation Y such that the MSE is minimum. Lifting Wavelet Transforms decomposes the image into different frequency subbands. Small coefficients in the subbands are dominated by noise while coefficients with large absolute value carry more image information than noise. Replacing noisy coefficients by zeros and an inverse lifting wavelet transform may lead to reconstruction that has lesser noise. Normally hard thresholding and soft thresholding techniques are used for denoising.

Hard Thresholding

$$D(X,T) = X \text{ if } |X| \rangle T$$
$$= 0 \text{ if } |X| \langle T$$

(30)

Soft Thresholding

$$D(X, T) = \text{Sign}(X) * \max(0, |X| - T)$$

(31)

Where X is the input subband, D is the denoised band after thresholding and T is the threshold level. The denoising algorithms, which are based on thresholding suggests that each coefficient of every detail subband is compared to threshold level and is either retained or killed if its magnitude is greater or less respectively.

In lifting wavelet transform decomposes an image into one approximate (LL) and three details (LH, HL and HH) subbands. The approximate coefficients are not submitted in this process. Since on one hand they carry the most important information about the image, on the other hand the noise mostly affects the high frequency subbands. Hence the HH subband contains mainly noise.

For estimating the noise level we use the Median Absolute Deviation (MAD) as proposed by Donoho [23].

$$\sigma = \frac{Median\left|Y_{ij}\right|}{0.6745}, Y_{ij} \in LH, HL, HH \tag{32}$$

The factor 0.6745 in the denominator rescales the numerator so that σ is also a suitable estimator for standard deviation for Gaussian white noise. Selecting an optimum threshold value (T) for soft thresholding is not an easy task. An optimum threshold value should be selected based on the subband characteristics. In lifting schemes subbands decomposition as the level increases, the coefficient of the subband becomes smoother. For example when an image is decomposed into 2 level LWT using Daubechies 4 tap lifting wavelet transform, we get four subbands figure (5), the HH subband of first level contains large amount of noise, hence the noise level is estimated for the HH subband using Eq (32).Once the noise level is estimated we select the threshold value T. The Threshold value T is

$$T = \sigma \cdot \left(\left|HM - GM\right|\right) \tag{33}$$

Here σ is the noise variance of the corrupted image. As given in [19], the Harmonic mean and geometric mean are best suited for the removal of Gaussian noise, hence we use the absolute difference of both the Harmonic Mean (HM) and Geometric Mean (GM) or either of the means also can be considered for denoising the image corrupted by Gaussian noise. The harmonic mean filter is better at removing Gaussian type noise and preserving edge features than the arithmetic mean filter. Hence we have considered harmonic mean than arithmetic mean. The process is repeated for LH and HL bands and threshold is selected for all the three bands once threshold is estimated, soft thresholding of Eq.(31) , is performed to denoise the image.

$$HM = \frac{M^2}{\sum\limits_{i=1}^{M} \sum\limits_{j=1}^{M} \frac{1}{g(i,j)}} \tag{34}$$

$$GM = \left[\prod\limits_{i=1}^{M} \prod\limits_{j=1}^{M} g(i, j)\right]^{\frac{1}{M^2}} \tag{35}$$

5.3. Proposed Adaptive Interpolation for Super Resolution Reconstruction

Once the image are denoised using our proposed soft thresholding technique, interpolation is performed to obtain an image of double, quadruple the size of the original image. Our proposed algorithm works in four phases: In the first phase the lifting wavelet transform based fused image is expanded. Suppose the size of the fused image is n x m. The image will be expanded to size N (2n-1) x (2m-1). In the figure (7) solid circles show original pixels and hallow circles show undefined pixels. In the remaining three phases these undefined pixels will be filled
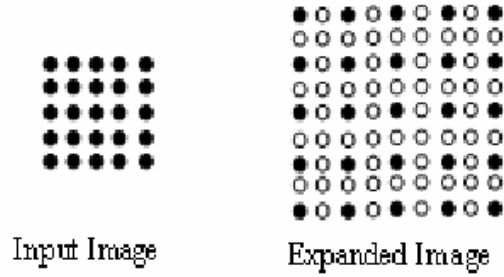
FIGURE 7: High Resolution Grid

The second phase of the algorithm is most important one. In this phase the interpolator assigns value to the undefined pixels
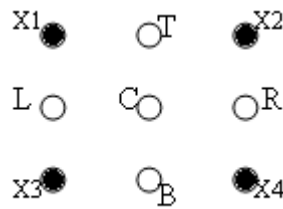

FIGURE 8 : HR unit cell with undefined pixels Top, Center, Bottom, Left, Right dented by T,C,B,L,R.

The undefined pixels are filled by following mutual exclusive condition.
Uniformity: select the range (X_1, X_2, X_3, X_4) and a Threshold T.

if range $(X_1, X_2, X_3, X_4) < \text{T}$ Then

$$C = \frac{(X_1 + X_2 + X_3 + X_4)}{4}$$

(36)

if there is edge in NW-SE Then

$\quad$ C=$(X_1 + X_2)/2$

if there is edge in NS Then

$\quad$ T=$(X_1 + X_2)/2$ and B =$(X_3 + X_4)/2$

if there is edge in EW Then

$\quad$ L=$(X_1 + X_3)/2$ and R =$(X_2 + X_4)/2$

(37)

In this phase, approximately 85% of the undefined pixels of HR image are filled. In the third phase the algorithm scans magnified image line by line and looking for those pixels which are left undefined in the previous phase.
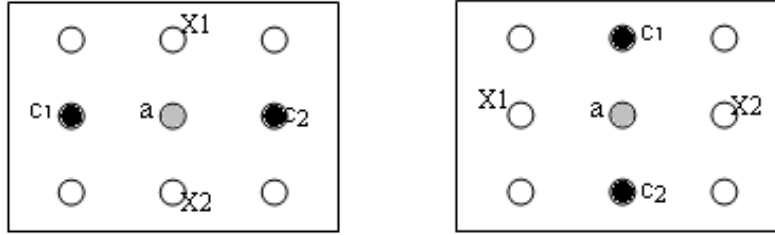
FIGURE 9 : Layout referred in the phase 3

In the third phase ,the algorithm checks for the layout as shown in Figure(9).

$$if \text{ there is edge } c_1c_2 \text{ then a}=(c_1 + c_2)/2$$

$$else \text{ } if \text{ there is edge } X_1X_2 \text{ then a}=(X_1 + X_2)/2$$

(38)

In the fourth phase all the undefined pixels will be filled. If there are any undefined pixels left then the median of the neighboring pixels is calculated and assigned. We call our interpolation method adaptive as the interpolator selects and assigns the values for the undefined pixels based on mutual exclusive condition.

6. PROPOSED ALGORITHM FOR SUPER RESOLUTION RECONSTRUCTION OF LOW RESOLUTION MAMMOGRAM IMAGES.

Our proposed novel super resolution reconstruction consists of following consecutive steps:

Step 1: Three input low resolution blurred, noisy, under sampled, rotated, shifted images are considered.

i.e. $I_1(i, j)$, $I_2(i, j)$, $I_3(i, j)$ where i=1…N , j=1….N   (39)

Step 2: The images are first preprocessed, i.e. registered using FFT based algorithm, as explained in section (5.1).

Step 3: The registered low resolution images are decomposed using LWT to a specified number of levels. At each level we will have one approximation i.e. LL sub band and 3 detail sub bands, i.e. LH, HL, HH coefficients.

Step 4: The decomposed images are fused using the fusion rule i.e. Maximum Frequency Fusion: "fusion by averaging for each band of decomposition and for each channel the wavelets coefficients of the three images is averaged". That is maximum frequencies of approximate and detail coefficients are fused separately

$$A_j^o I = \max(A_j^o I_1 + A_j^o I_2 + A_j^o I3)/3 \qquad D_j^s I = \max(D_j^s I_1 + D_j^s I_2 + D_j^s I_3)/3$$

(40)

Step 5: The fused image contains LL, LH, HL and HH subbands.

   a) Obtain the noise variance (σ) using Eq.(32) for LH, HL and HH subbands of level one.
   b) Compute Eq.(33) and select the threshold (T) for LH, HL and HH subbands of level 1.
   c) Denoise all the detail subband coefficients of level one (except LL) using soft thresholding given in Eq.(31) by substituting the threshold value obtained in step (5b).

Step 6: Most of the additive noise will be eliminated during the fusion process by denoising using our proposed soft hresolding approach as explained in section (5.2.1), where as the image is deblurred using Iterative Blind Deconvolution Algorithm (IBD)[30] .

Step 7: Inverse LWT is applied to obtain a high resolution restored image.

Step 8: Finally in order to obtain a super resolved image, an image with double the resolution as that of the original image our proposed adaptive interpolation as explained in section (5.3) is applied.

6.1. Quality Measurement

1) Improvement in Signal-to-Noise Ratio (ISNR)

For the purpose of objectively testing the performance of the restored image, Improvement in signal to noise ratio (ISNR) is used as the criteria which is defined by

$$ISNR = 10\log_{10} \frac{\sum_{i,j}\left[f(i,j)-y(i,j)\right]^2}{\sum_{i,j}\left[f(i,j)-g(i,j)\right]^2}$$

(41)

Where j and i are the total number of pixels in the horizontal and vertical dimensions of the image; f(i, j), y(i, j) and g(i, j) are the original, degraded and the restored image.

2) The MSE and PSNR of the Reconstructed Image is

$$MSE = \frac{\sum[f(i,j)-F(I,J)]^2}{N^2}$$

(42)

Where f(i, j) is the source image F(I,J) is the reconstructed image, which contains N x N pixels

$$PSNR = 20\log_{10}\left(\frac{255}{RMSE}\right)$$

(43)

3) Super Resolution Factor

$$SRF = \frac{\sum_{i=1}^{M}\sum_{j=1}^{N}\left(F(i,j)-f(i,j)\right)^2}{\sum_{i=1}^{M}\sum_{j=1}^{N}\left(y(i,j)-f(i,j)\right)^2}$$

(44)

4) MSSIM

The structural similarity (SSIM) index is defined in [27] by equations

$$SSIM(f,F)=\frac{(2\mu_f\mu_F+C_1)(2\sigma_F+C_2)}{(\mu_f^2+\mu_F^2+C_1)(\sigma_f^2+\sigma_F^2+C_2)}$$

(45)

Liyakathunisa & C.N. Ravi Kumar

$$MSSIM(f,F)=\frac{1}{G}\sum_{p=1}^{G}SSIM(f,F)$$ (46)

The Structural SIMilarity index between the original image and reconstructed image is given by SSIM, where μ_f and μ_F are mean intensities of original and reconstructed images, σ_f and σ_F are standard deviations of original and reconstructed images, f and F are image contents of pth local window and G is the number of local windows in the image.

7. EXPERIMENTAL RESULTS AND DISCUSSIONS.
To evaluate the performance of the proposed algorithm we performed our experiments using MATLAB software. The tested images were selected from "**Geneva Foundation for Medical Education and Research**". The test data can be summarized as follows
Case1: Ductal carcinoma in Situ.
Case 2: Fat necrosis of breast- benign inflammatory
Case 3: Benign tubular adenomyoepithelioma
Case 4: clustered micro calcification masses.

Each data set consists of three to four LR mammographic images generated from a reference image. To simulate low resolution and low dosage conditions, each LR mammographic image is generated by applying a motion blur with an angel of (10, 20 and 30) and Gaussian white noise with SNR(5, 10,15 and 20 dB) is added to the blurred low resolution images. The goal is to generate a Super Resolution image of size 512 x512 and 1024x1024 from three noisy, blurred, under sampled and mis-registered images. In addition a comparative study has been made with well known algorithms like; Projection on to Convex Sets(POCS), Papoulis Gerchberg (PG) Algorithm, Iterative Back Projection(IBP) and DWT based SRR[3]. Figures (11 & 12) show two different cases of LR mammograms and the super resolution results of our proposed algorithm compared with POCS, Papoulis, IBP and DWT. To asses the performance of the super resolution model on test images, we used the above mentioned metrics to estimate the enhancement quality based on PSNR, ISNR, SRF and MSSIM measure. Table 1 and Table 2, show a comparative study of our algorithm with POCS, Papoulis Gerchberg(P.G), Iterative Back Projection(IBP) and DWT in terms of PSNR, ISNR and MSSIM values.

The results indicate that our proposed super resolution reconstruction have much more high frequency information than Projection on to Convex Sets, Papoulis Gerchberg Algorithm and Iterative Back Projection. To evaluate the performance of the proposed method in a quantitative manner , PSNR is computed for the resolution enhanced images obtained with tested algorithms, relative to the reference image used to generate the lo w resolution images. The PSNR results for all the test cases are summarized in Table 1. It can be observed that the PSNR values for the mammographic images generated using the proposed method are noticeably higher than those produced using the other methods. Case 1 and Case 2 are shown in figures (11 & 12) respectively.

case 1: is mammogram of Ductal carcinoma in Situ (DCIS), the carcinomas are difficult to interpret in the high resolution mammographic images obtained using POCS, PG and IBP. Both wavelet based SRR and LWT SRR method provide noticeably improved structural detail. The proposed LWT based SRR provides an improved structural contrast when compared to wavelet based SRR.

In case 2, mammogram of 69-year-old woman with benign tubular adenomyoepithelioma is considered, it's a Lateral oblique mammogram showing circumscribed mass lying inferiorly in left breast. Benign calcifications are also present. The calcification behind the dense tissues is very difficult to interpret in the high resolution mammographic images obtained using POCS, PG and IBP. But the wavelet based SRR and LWT based SRR provide noticeably improved structural

detail pertaining to the calcification. Lifting wavelet based SRR provides an improved contrast and a sharper image of the masses. The shape, boundaries and structure of the masses tend to be better defined in the high resolution image provided by the proposed method.

The MSSIM and ISNR results are summarized in Table 2, MSSIM which accounts well for texture changes introduced by super resolution process, has its value increased for the proposed lifting wavelet based approach. MSSIM was created to reflect the perceived visual quality by humans [27][33].
From the Table II , it is clear that the proposed LWT SRR algorithm increases the perceptual visual quality. Another interesting factor is that the proposed Lifting Wavelet based SRR have much more detail information than the results of Projection on to Convex Sets, Papoulis Gerchberg Algorithm and Iterative Back Projection.

From the Table (1 and 2) and Figures (11 & 12), we observe that the proposed algorithm outperforms the others, and we have a clearer and high resolution mammogram with a super resolution factor of 4, much better than the original one, which is very helpful for the radiologist to make proper decision whether it is benign or malignant characteristics of breast tumor. Once the exact location of the tumor is detected, radiation can be passed in the precise location, by which we can avoid the health risks of the patients and side effect of radiation therapy can be avoided. And from the plots in figure(13) it's clear that our proposed approach has better ISNR and MSSIM when compared to other approaches.

Image	POCS SRR		Papoulis Gerchberg (P G) SRR		IBP SRR		DWT based SRR[3]		Proposed LWT SRR	
	MSE	*PSNR*	*MSE*	*PSNR*	*MSE*	*PSNR*	*MSE*	*PSNR*	*MSE*	*PSNR*
case 1	34.87	32.7	32.5	33.1	50.43	37.1	59.63	51.043	16.76	62.23
case 2	69.46	29.71	67.48	29.83	69.46	29.73	42.66	54.11	25.46	58.46
case 3	54.11	30.79	53.45	30.85	40.37	28.59	28.81	57.056	11.98	65.14
case 4	34.21	32.78	30.61	33.27	37.6	32.37	54.94	49.42	40.71	52.02

TABLE I: MSE and PSNR comparison of our proposed approach with other approaches

| Image	POCS SRR		Papoulis Gerchberg (P G) SRR		IBP SRR		DWT based SRR[3]		Proposed LWT SRR	
	ISNR	*MSSIM*	*ISNR*	*MSSIM*	*ISNR*	*MSSIM*	*ISNR*	*MSSIM*	*ISNR*	*MSSIM*
case 1	2.41	0.67	2.78	0.69	2.82	0.68	6.82	0.897	13.61	0.99
case 2	3.7	0.63	3.49	0.67	3.61	0.67	6.78	0.890	13.61	0.985
case 3	2.98	0.66	3.21	0.71	3.23	0.69	6.83	0.912	9.46	0.971
case 4	3.7	0.73	3.17	0.68	3.56	0.71	7.12	0.870	8.29	0.984

TABLE II: ISNR and MSSIM comparison of our proposed approach with other approaches

(a)

(b)

(c)

(d)
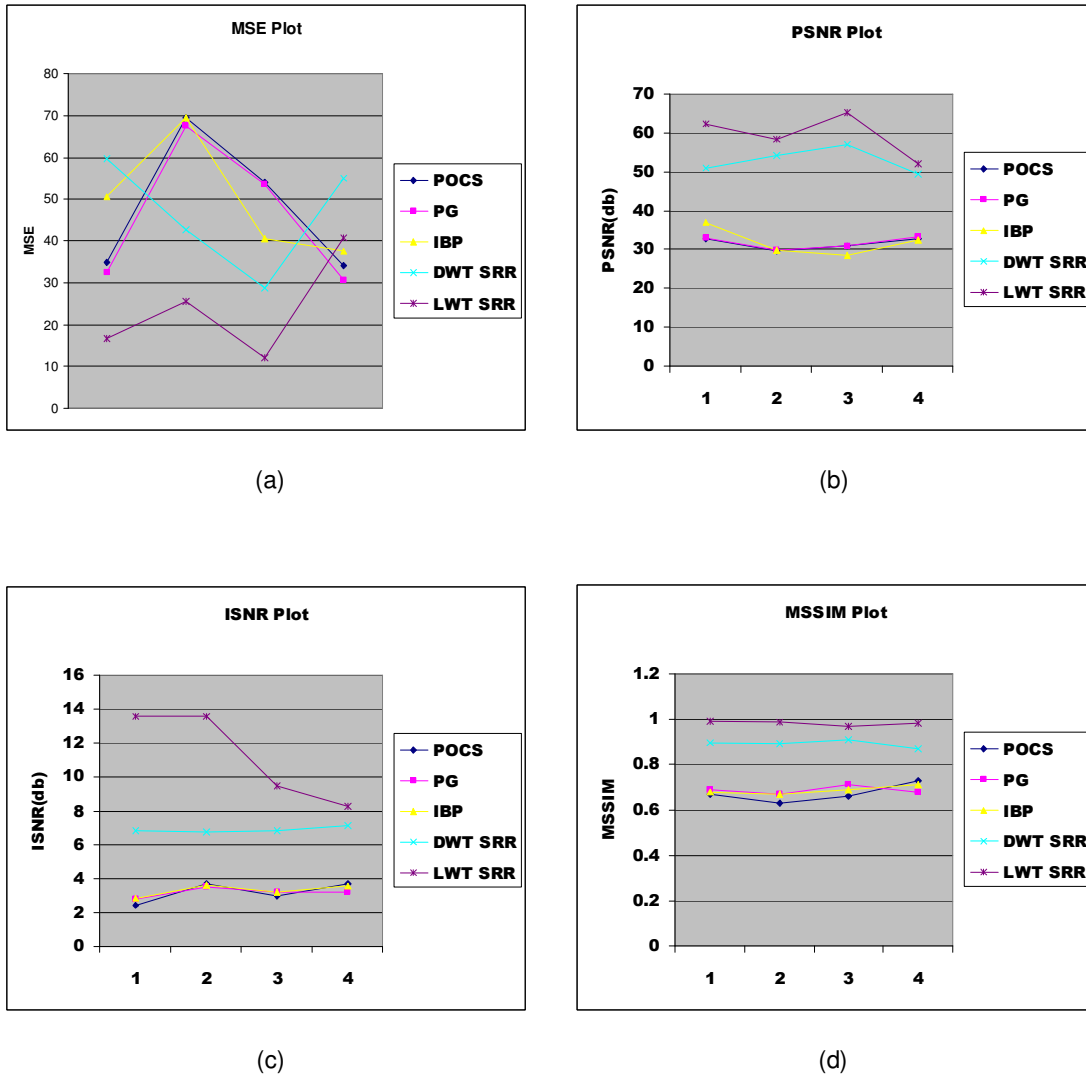
FIGURE 10: (a) Comparison graph of MSE at different blur and noise densities of LR mammogram images (b) Comparison graph of PSNR at different blur and noise densities of LR mammogram images. (c) Comparison graph of ISNR at different blur and noise densities of LR images (d) Comparison graph of MSSIM at different blur and noise densities of LR images

7.1 Simulation Results

Case 1: Ductal carcinoma in situ (DCIS) mammogram with a Super resolution factor of 2 (enlarged from 256x256 to 512 by 512)
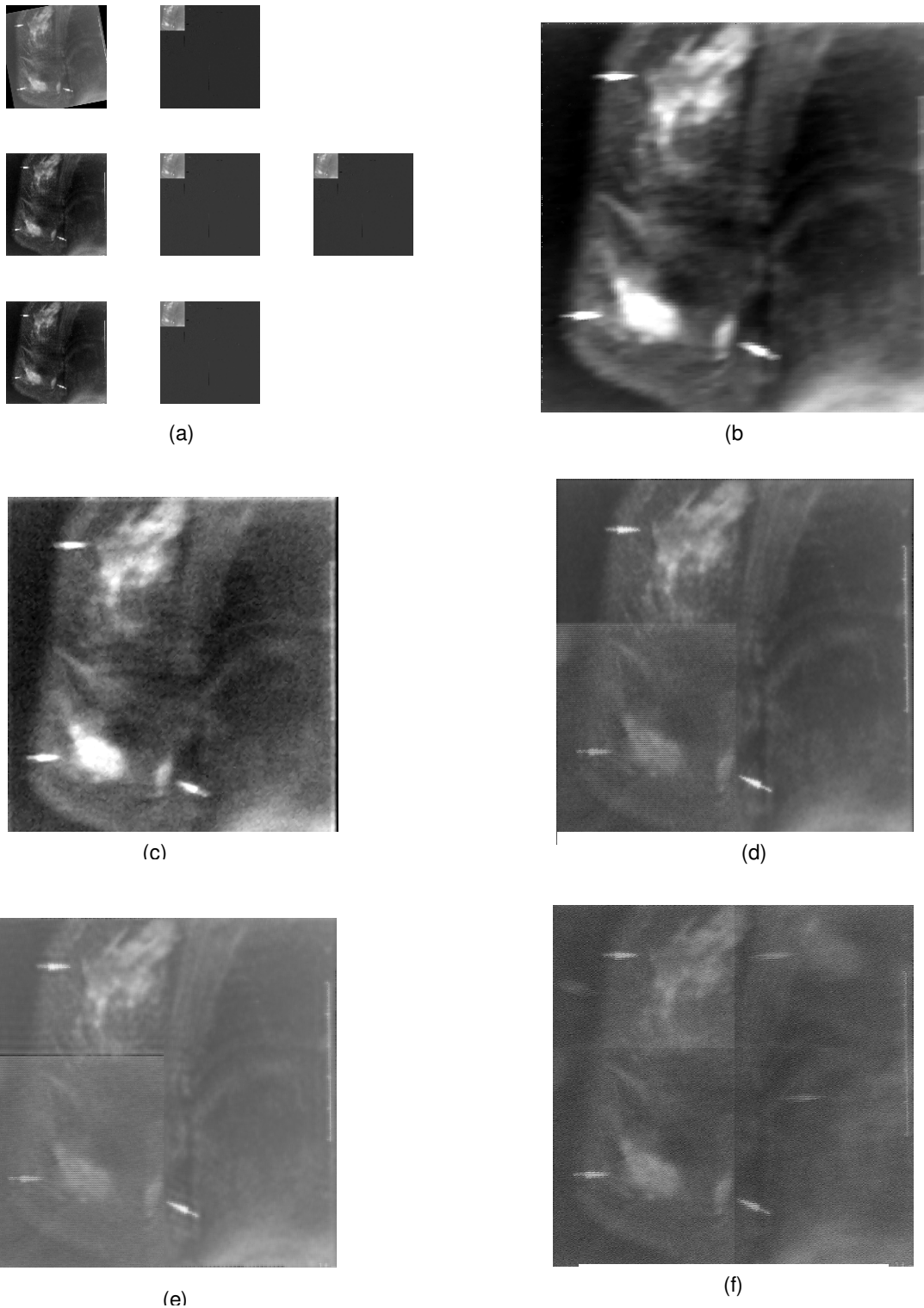
FIGURE 11: (a) Low Resolution Images (b) Proposed LWT based SRR   (c) DWT based SRR
(d) POCS SRR   (e) Papoulis Gerchberg SRR   (f) IBP SRR

Case 2: 69-year-old woman with benign tubular adenomyoepithelioma with a super resolution factor of 4(enlarged from 256 x 256 to 1024 x 1024)
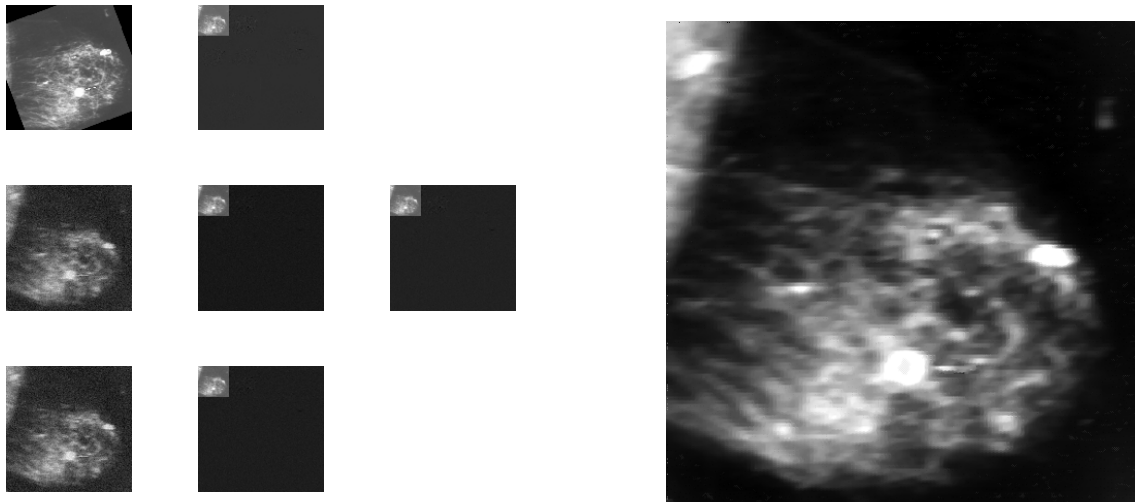
(a)

(b)
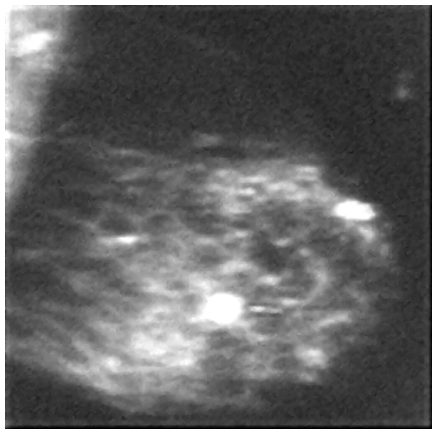
(c)
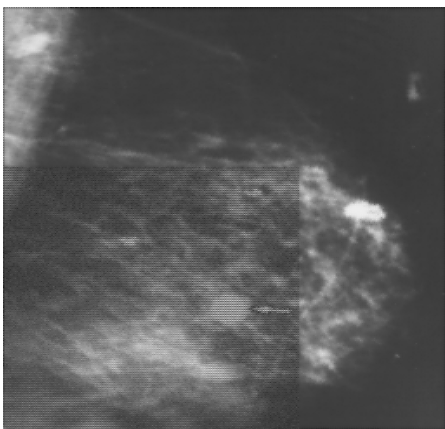
(d)
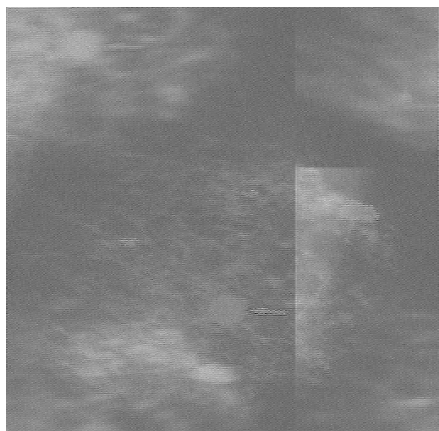
(e)
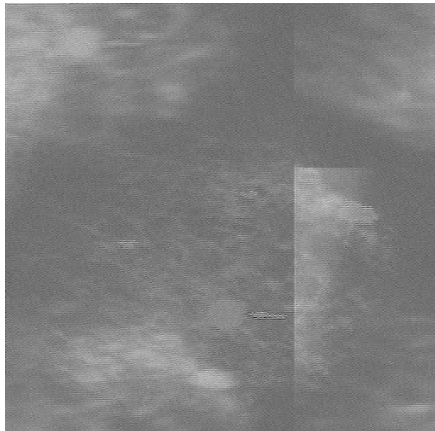
(f)

FIGURE 12: (a) Low Resolution Images (b) Proposed LWT based SRR (c) DWT based SRR
(d) POCS SRR (e) Papoulis Gerchberg SRR (f) IBP SRR

8. CONCLUSION

In this paper we have proposed a novel and efficient lifting scheme based denoising for super resolution reconstruction of low resolution mammogram images. We have presented a new way to improve the quality of x-ray mammography images without having to use more radiations, which increases health risks of patients. The results indicate that the proposed system can facilitate the doctor to detect breast cancer in early stage of diagnosis process. Early detection tests for breast cancer can save many thousands of lives, with super resolution reconstruction the cancer can be diagnosed at an early stage and treated successfully. High resolution images give better visibility of the breast, particularly near the skin line, chest wall and in women with dense breast tissues. As medical imaging moves towards complete digital imaging and produces prohibitively large amounts of data, compression is necessary for storage and communication purposes. Our method has the potential for storage and communication purposes. Our method has the potential to eliminate the need to store images at full resolution, since they could be regenerated them from low resolution ones. Experimental results show that the proposed algorithm yields significantly superior image quality when it is compared to the other well known algorithms.

REFERENCES

[1] Liyakathunisa and C.N.Ravi Kumar, "Advances in Super Resolution Reconstruction of Low Resolution Images" International Journal of Computational Intelligence Research ISSN 0973-1873 Volume 6, Number 2 , pp. 215-236,2010.

[2] Liyakathunisa, C.N.Ravi Kumar and V.K. Ananthashayana , "Super Resolution Reconstruction of Low Resolution Images using Wavelet Lifting schemes" in Proc ICCEE'09, 2nd International Conference on Electrical Computer Engineering", Dec 28-30TH 2009, Dubai, Indexed in IEEE Xplore.

[3] Liyakathunisa and C.N.Ravi Kumar, "A Novel and Robust Wavelet Based Super Resolution Reconstruction of Low Resolution Images Using Efficient Denoising and Adaptive Interpolation", in International Journal of Image Processing-IJIP, CSC Journals Publications, Issue 4, Vol 4, pp 401-420, 2010.

[4] R.Gaughan, "New approaches to early detection of breast cancer makes small gains" ,Biophotonics Int. , pp 48-53, 1998.

[5] Smith R.A., "Epidemiology of breast cancer categorical course in physics", Tech. Aspects Breast Imaging, Radiol. Sco. N. Amer., pp 21-33, 1993.

[6] S. Shapiro, W. Venet, P.Strax, L.Venet, and R. Roester, " Ten-to Fourteen year Effect of screening on breast cancer mortality", JNCL, vol 69, pp 349, 1982.

[7] M. Irani and S. Peleg, "Improving resolution by image registration", CVGIP: Graphical Models and Image Proc., vol. 53, pp. 231-239, May 1991.

[8] R.Y. Tsai and T.S. Huang, "Multiple frame image restoration and registration", in Advances in Computer Vision and Image Processing. Greenwich, CT: AI Press Inc., pp, 317-339.

[9] P. Vandewalle, S. Susstrunk, and M. Vetterli, Lcav, "A frequency domain approach to registration of aliased images with application to Super resolution", EURASIP Journal on applied signal processing pp 1-14, 2006.

[10] S. C. Park, M. K. Park, and M. G. Kang, "Super-resolution image reconstruction: A technical review", IEEE Signal Processing Mag., vol. 20, pp. 21-36, May 2003.

[11] H. Greenspan, G. Oz, N. Kiryati, and S. Peled, "Super-resolution in mri," in Proceedings of IEEE International Symposium on Biomedical Imaging, pp. 943 -946, 2002.

[12] J. A. Kennedy, O. Israel, A. Frenkel, R. Bar-Shalom, and H. Azhari, "Super-resolution in pet imaging", IEEE transactions on medical imaging, vol. 25, no. 2, pp. 137 - 147, February 2006.

[13] J. T. Hsu1, C. C. Yen, C. C. Li, M. Sun, B. Tian, and M. Kaygusuz, "Application of wavelet-based pocs super resolution for cardiovascular mri image enhancement ", in Proceedings of the Third International Conference on Image and Graphics (ICIG04), pp. 572-575, 2004.

[14] Alexander wong and Jacob Scharcanski, " Phase -adaptive Super Resolution of mammogram Images using complex wavelts ", 2009.

[15] Jun Zhang, olacFuentes and Ming-Yingleung, "Super resolution of Mammograms", 2010.

[16] A.Jensen, A.la Cour-Hardo, "Ripples in Mathematics" , Springer publications.

[17] Barbara Zltova, J.Flusser, "Image Registration: Survey", Image and vision computing, 21, Elsevier publications, 2003.

[18] E.D. Castro, C. Morandi, "Registration of translated and rotated images using finite Fourier transform" , IEEE Transactions on Pattern Analysis and Machine Intelligence 700–703, 1987.

[19] Gonazalez Woods , " Digital Image Processing", 2nd Edition.

[20] S. Grace Chang, Bin Yu and M. Vattereli, "Adaptive Wavelet Thresholding for Image denoising and compression", IEEE Transaction, Image Processing, vol. 9, pp. 1532-15460.

[21] S.K.Mohiden, Perumal,Satik, "Image Denosing using DWT", IJCSNS, Vol 8, No 1, 2008.

[22] D. Gnanadurai, V.Sadsivam, "An Efficient Adaptive Threshoding Technique for Wavalet based Image Denosing" , IJSP, Vol 2, spring 2006.

[23] D.L.Donoho and I.M JohnStone, "Adapting to unknown smoothness via wavelet shrinkage ", Journal of American Association, Vol 90,no, 432, pp1200-1224 .

[24] Huang, X.S., Chen, Z, "A Wavelet-Based Image Fusion Algorithm" , In Proceedings of the IEEE Region 10 Conference on Computers, Communications, Control and Power Engineering (TENCON 2002), 602-605, Beijing 2002.

[25] T. Acharya, P.S. Tsai, "Image up-sampling using Discrete Wavelet Transform", in Proceedings of the 7th International Conference on Computer Vision, Pattern Recognition and Image Processing (CVPRIP).

[26] S. Grace Chang, Bin Yu and M. Vattereli, "Adaptive Wavelet Thresholding for Image denoising and compression", IEEE Transaction, Image Processing, vol. 9, pp. 1532-15460.

[27] Wang, Bovik, Sheikh, et al, "Image Quality Assessment: From Error Visibility to Structural Similarity", IEEE Transactions of Image Processing, vol. 13, pp. 1-12, April 2004.

[28] S. Chaudhuri, Ed., "Super-Resolution Imaging", Norwell, A: Kluwer, 2001.

[29] S.Susan Young, Ronal G.Diggers, Eddie L.Jacobs, "Signal Processing and performance Analysis for imaging   Systems", ARTEC HOUSE, INC , 2008.

[30] G.R.Ayer and J.C.Danity, " Iterative Blind Deconvolution", vol13, No 7, optics Letters, July 1988.

[31] G.K. Lemanur, Drocihe and J.Decoinck, "Highly Regular Wavelets for the Detection of clustered Micro calcification in Mammograms", IEEE Trans on Medical Imaging, VOl.22, No. 3, March 2003.

[32] J.Kristin , McLoughlin, J.Philip , Bones, "Noise Equalization for Detection of Micro calcification Clusters in Direct Digital Mammogram Images", IEE Trans on Medical Imaging, Vol 23, No 0 , March 2004.

[33] I. B´egin and F. P. Ferrie, "Comparison of super-resolution algorithms using image quality measures," in Proceedings of the 3rd Canadian conference on computer and robot vision. Washington, DC, USA: IEEE Computer Society, pp. 72, 2006.

[34] B. Girod, "What's wrong with mean-squared error?" in Digital images and human vision, MIT Press, Cambridge, MA. ISBN 0-262-23171-9, pp. 207–220, 1993.